NJC

Accepted Manuscript

This is an *Accepted Manuscript*, which has been through the Royal Society of Chemistry peer review process and has been accepted for publication.

Accepted Manuscripts are published online shortly after acceptance, before technical editing, formatting and proof reading. Using this free service, authors can make their results available to the community, in citable form, before we publish the edited article. We will replace this *Accepted Manuscript* with the edited and formatted *Advance Article* as soon as it is available.

You can find more information about *Accepted Manuscripts* in the Information for Authors.

Please note that technical editing may introduce minor changes to the text and/or graphics, which may alter content. The journal's standard Terms & Conditions and the Ethical guidelines still apply. In no event shall the Royal Society of Chemistry be held responsible for any errors or omissions in this *Accepted Manuscript* or any consequences arising from the use of any information it contains.

ROYAL SOCIETY OF CHEMISTRY

www.rsc.org/njc

Journal Name

RSCPublishing

ARTICLE

Pd Complex of a NNN Pincer Ligand Supported on γ-Fe_2O_3@SiO_2 Magnetic Nanoparticles: A New Catalyst for Heck, Suzuki and Sonogashira Coupling Reactions

Cite this: DOI: 10.1039/xoxxoooooox

Received ooth January 2015,
Accepted ooth January 2015

DOI: 10.1039/xoxxoooooox

www.rsc.org/

Sara Sobhani[a]* Zohre Zeraatkar[a], Farzaneh Zarifi[a]

In this paper, Pd complex of bis(imino)pyridine as a NNN pincer ligand supported on γ-Fe_2O_3@SiO_2 magnetic nanoparticles (Pd-BIP-γ-Fe_2O_3@SiO_2) was synthesized and characterized by SEM, TEM, FT-IR, TGA, ICP, XRD, XPS, VSM and elemental analysis. The synthesized catalyst was used successfully as a new air- and moisture-stable phosphine-free Pd catalyst for Heck, Suzuki and Sonogashira coupling reactions of aryl iodides, bromides and chlorides with alkyl acrylates, styrene, phenylboronic acid and phenylacetylene. The true heterogeneous magnetically recyclable catalyst can be separated easily by a magnetic bar and reused ten times without any drastic loss of its catalytic activity.

Introduction

Heck, Suzuki and Sonogashira cross-coupling reactions are important strategies for the formation of carbon-carbon bonds and catalyzed originally by homogeneous Pd catalyst.[1] However, these reactions suffer from problems associated with the separation and recovery of the homogeneous and high cost Pd catalyst, which might result in undesirable metal contamination of the products. Therefore, to have an efficient recovery and recycling of Pd catalyst, the immobilization of homogeneous Pd catalytic systems on different supporting materials has been the subject of intense research.[2] Other challenge facing this field is the design of the catalysts that are more robust and efficient using valuable ligands as stabilizers for Pd species.[3] During the past decades, the most common ligands used for these cross-coupling reactions have been the phoshine-based ones.[4] Most of the phosphine-based ligands are air and/or moisture-sensitive, poisonous, unrecoverable and degradable at elevated temperature which limited their large-scale application in the industrial chemistry.[5] In recent years, several groups have tried to develop phosphine-free Pd complexes for cross-coupling reactions. However, the reported complexes have the drawbacks of requiring an excess of expensive ligands, multistep syntheses and inert conditions. Moreover, most of the reported methods are amenable only for the cross-coupling reactions of aryl iodides and bromides.[6]

Bis(imino)pyridines (BIP) with the central nitrogen donor and flanking imine arms are known as NNN tridentate pincer ligands, which coordinate easily with transition metals such as Mn, Zn, Gd, Ni, Co and Fe to form metal complexes.[7] These metal complexes have mainly applied as highly active and selective catalysts for the oligo- and polymerization of olefins.[8] Metal complexes containing nitrogen donor pincer ligands present a high stability due to the formation of two five-membered metallacycles with a tridentate nitrogen ligand.[9] Moreover, pincer ligands offer high stability towards heat, air and moisture and great control of the steric and electronic properties of metal centers.[10] Recently, synthesis and application of a complex of BIP with Pd supported on MCM-41 in Suzuki coupling reaction was reported.[11] Despite the high catalytic activity of this heterogeneous palladium catalyst, its separation technique was energy and time consuming. Moreover, the catalyst was used for the coupling reaction of only aryl bromides as aryl halides with phenylboronic acid. Employing magnetic nanoparticles (MNPs) as a support for Pd complex can solve the problem of catalyst separation. This kind of supporting allows Pd catalyst to be easily separated from the reaction medium by application of an external permanent magnet. Magnetic separation of MNPs, which is an alternative to filtration or centrifugation, prevents loss of the catalyst, and saves time and energy.[12] However, MNPs are readily aggregated due to the self interactions. In order to prevent the aggregation, the surface of MNPs was usually modified with suitable coating such as silica layer.[13] The outer shell of silica not only improves the dispersibility but also provides suitable sites (Si-OH groups) for further surface functionalization.[14]

To benefit the valuable applications of MNPs and unique properties of BIP as a NNN pincer ligand, and in continues of our recent works on the development of heterogeneous catalysts in organic transformations,[15] herein, we report the synthesis of an air- and moisture-stable phosphine-free Pd complex with BIP supported on γ-Fe_2O_3@SiO_2 nanoparticles (Pd-BIP-γ-Fe_2O_3@SiO_2). The synthesized catalyst was characterized by different methods such as TEM (transmission electron microscopy), SEM (scanning electron microscope), FT-IR (Fourier transform infrared spectroscopy), TGA (Thermogravimetric analysis), ICP (inductively coupled plasma), XRD (X-ray diffraction), XPS (X-ray photoelectron

spectrum), VSM (Vibrating Sample Manetometer) and elemental analysis and used as a new magnetically recoverable Pd catalyst for the carbon–carbon coupling reactions of aryl halides with olefines, phenylboronic acid and phenylacetylene *via* Heck, Suzuki and Sonogashira reactions.

Results and discussion

Synthesis and characterization of Pd-BIP-γ-Fe_2O_3@SiO_2

Synthesis of Pd-BIP-γ-Fe_2O_3@SiO_2 is schematically described in Scheme 1. The synthesized silica-coated γ-Fe_2O_3 nanoparticles (γ-Fe_2O_3@SiO_2)[16] were functionalized with 3-aminopropyltriethoxysilane by refluxing in dry toluene. The obtained amino-functionalized γ-Fe_2O_3@SiO_2 reacted with pyridine-2,6-dicarbaldehyde to produce γ-Fe_2O_3@SiO_2 supported with bis(imino)pyridine (BIP-γ-Fe_2O_3@SiO_2). Pd complex of BIP supported on γ-Fe_2O_3@SiO_2 (Pd-BIP-γ-Fe_2O_3@SiO_2) was synthesized by refluxing BIP-γ-Fe_2O_3@SiO_2 with $Pd(OAc)_2$ in methanol. The synthesized Pd-BIP-γ-Fe_2O_3@SiO_2 was fully characterized by SEM, TEM, TGA, FT-IR, ICP, XRD, XPS, VSM and elemental analysis.

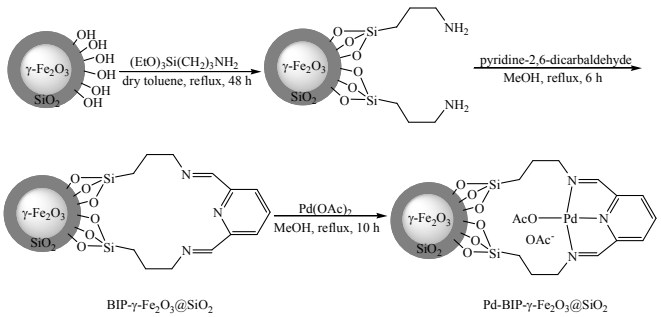

Scheme 1. Synthesis of Pd-BIP-γ-Fe_2O_3@SiO_2

According to the SEM (Fig. 1), it was observed that the synthesized Pd-BIP-γ-Fe_2O_3@SiO_2 has uniformity and spherical morphology. TEM images of Pd-BIP-γ-Fe_2O_3@SiO_2 displayed a dark γ-Fe_2O_3 core surrounded by a gray silica shell with thickness of about 4 nm. It can be seen that the NPs are spherical in shape and relatively monodispersed. The particle size distribution of Pd-BIP-γ-Fe_2O_3@SiO_2 was evaluated using TEM and showed that the average diameter of the particles was 20 nm.

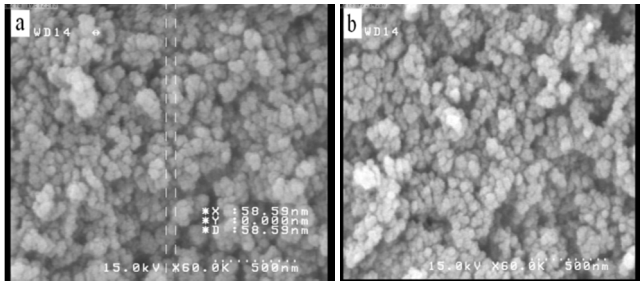

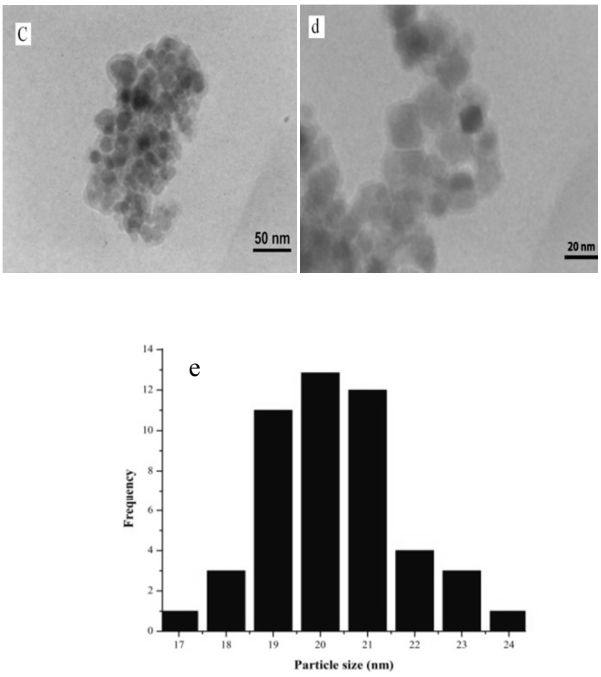

Figure 1. (a,b) SEM images, (c,d) TEM images and (e) particle size distribution histogram of Pd-BIP-γ-Fe_2O_3@SiO_2

FT-IR spectra of amino-functionalized γ-Fe_2O_3@SiO_2, BIP-γ-Fe_2O_3@SiO_2 and Pd-BIP-γ-Fe_2O_3@SiO_2 are shown in Figure 2. The bands at around 565-684, 1048-1206 and 2935 cm^{-1} were assigned to the stretching vibrations of Fe-O, Si-O and CH_2 bonds, respectively. The peak positioned at around 1471 cm^{-1} in the FT-IR spectrum of amino-functionalized γ-Fe_2O_3@SiO_2 was related to the bending of the CH_2 bonds. The characteristic absorption bands due to the stretching vibration of C=C and C=N were observed at 1409-1454 and 1646 cm^{-1} in the spectrum of BIP-γ-Fe_2O_3@SiO_2. Peaks appeared at 1634 and 1401 cm^{-1} in the spectrum of Pd-BIP-γ-Fe_2O_3@SiO_2 were related to COO (in acetate) and confirmed the presence of Pd in the catalyst.

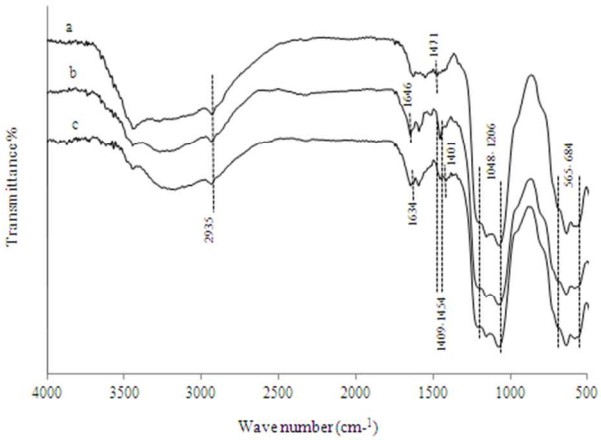

Figure 2. FT-IR spectra of (a) amino-functionalized γ-Fe_2O_3@SiO_2, (b) BIP-γ-Fe_2O_3@SiO_2 and (c) Pd-BIP-γ-Fe_2O_3@SiO_2

FT-IR spectra of BIP-γ-Fe_2O_3@SiO_2 and Pd-BIP-γ-Fe_2O_3@SiO_2 were compared with those of unsupported **1** and **2** (Scheme 2, Fig.

3). Comparison of FT-IR spectra of BIP-γ-Fe_2O_3@SiO_2 and Pd-BIP-γ-Fe_2O_3@SiO_2 with those of **1** and **2** showed that the characteristic peaks were positioned at the same wave numbers, but with a small shift in the spectrum of BIP-γ-Fe_2O_3@SiO_2 and Pd-BIP-γ-Fe_2O_3@SiO_2 due to the interaction with the support. As shown in Figure 3, the bands at around 1049-1110 and 2923 cm^{-1} were assigned to the stretching vibrations of Si-O and CH_2 bonds, respectively. The characteristic absorption bands related to the stretching vibration of C=C and C=N were observed at 1455 and 1648 cm^{-1} in the spectrum of **1**. After complexation with palladium, these two peaks in the spectrum of **2** were shifted to 1454 and 1641 cm^{-1}, respectively, because of the bond formation between the metal and the ligand. The overlap of these peaks with the COO peak in acetate causes them to become broad.

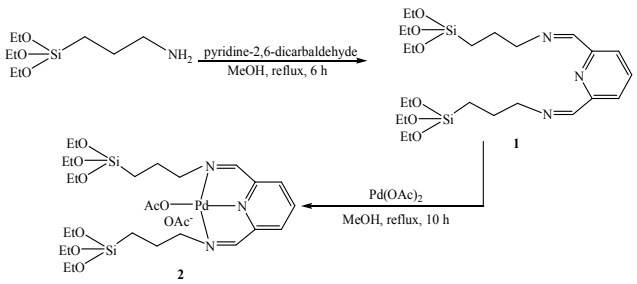

Scheme 2. Synthesis of **1** and **2**

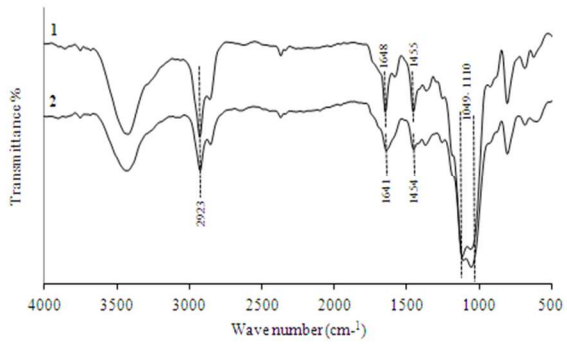

Figure 3. FT-IR spectra of **1** and **2**

The thermal behaviour of BIP-γ-Fe_2O_3@SiO_2 is shown in Figure 4. A significant decrease in the weight percentage at about 145 °C was related to the desorption of water molecules from surface. This was evaluated to be ~0.5% according to the TGA. Another decreasing peak started at 234 °C. The organic parts decomposed completely at around 550 °C. According to the TGA, the amount of BIP functionalized on γ-Fe_2O_3@SiO_2 calculated to be 0.34 $mmol.g^{-1}$. These results are in good agreement with the elemental analysis data (N = 1.58% and C = 4.96%). The ICP analysis of Pd-BIP-γ-Fe_2O_3@SiO_2 showed that 0.28 mmol of Pd was loaded on 1 g of the catalyst.

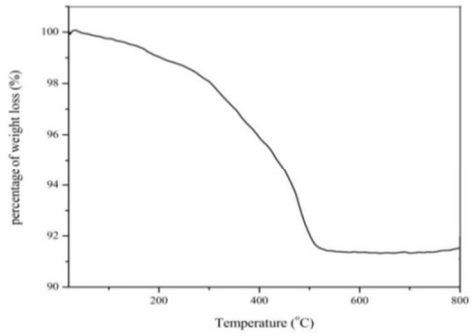

Figure 4. TGA diagram of BIP-γ-Fe_2O_3@SiO_2

As presented in Figure 5, the reflection planes of (2 2 0), (3 1 1), (4 0 0), (4 2 2), (5 1 1) and (4 4 0) at 2θ = 30.3°, 35.7°, 43.4°, 53.8°, 57.4° and 63.0° were readily recognized from the XRD pattern of γ-Fe_2O_3. The same set of characteristic peaks was observed in the XRD pattern of Pd-BIP-γ-Fe_2O_3@SiO_2, which indicates the stability of the crystalline phase of nanoparticles during the subsequent surface modification. The observed diffraction peaks was indicated that γ-Fe_2O_3 NPs mostly exist in face-centered cubic structure. XRD pattern of Pd-BIP-γ-Fe_2O_3@SiO_2 showed a weak peak at 2θ = 39.9° correspond to (1 1 1) reflection of the supported Pd. This peak is relatively broad due to the small particle size of the Pd NPs.[17]

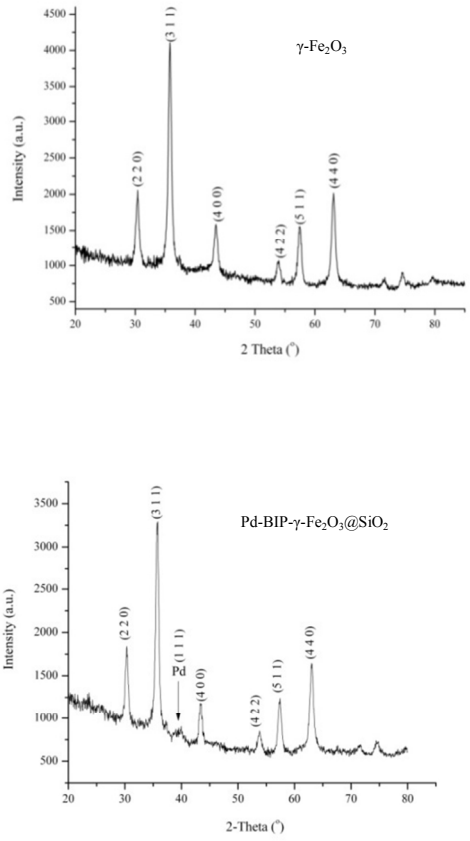

Figure 5. XRD patterns of γ-Fe_2O_3 and Pd-BIP-γ-Fe_2O_3@SiO_2

X-ray photoelectron spectroscopy (XPS) was carried out to establish the oxidation state of Pd in the catalyst (Fig. 6). The binding energies

at 337.6 and 342.1 eV corresponding to Pd $3d_{5/2}$ and Pd $3d_{3/2}$, respectively, confirmed the presence of Pd (II) in the catalyst. No peaks corresponding to Pd (0) in the metallic state was detected.

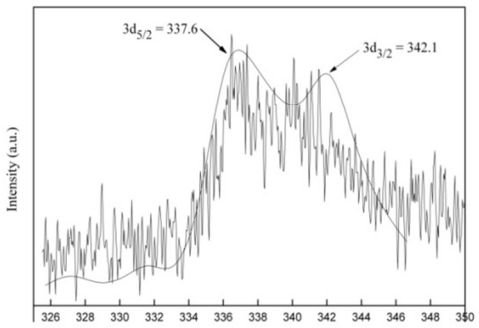

Figure 6. X-ray photoelectron spectroscopy (XPS) of Pd-BIP-γ-Fe_2O_3@SiO_2

The magnetization curves of γ-Fe_2O_3 and Pd-BIP-γ-Fe_2O_3@SiO_2 were measured at room temperature with a vibrating sample magnetometry (VSM). As shown in Figure 7, the remanence and coercivity were reduced insignificantly, which indicates that both unmodified and Pd-BIP-modified γ-Fe_2O_3 are superparamagnetic. The value of saturation magnetic moments of γ-Fe_2O_3 decreased with the attachment of SiO_2 and the Pd-BIP from 68.6 emu/g to 53.0 emu/g for Pd-BIP-γ-Fe_2O_3@SiO_2. However, Pd-BIP-γ-Fe_2O_3@SiO_2 with superparamagnetic characteristics and high magnetization values can quickly respond to an external magnetic field and redisperse when the external magnetic field is removed. This supports their potential application for targeting and separation.

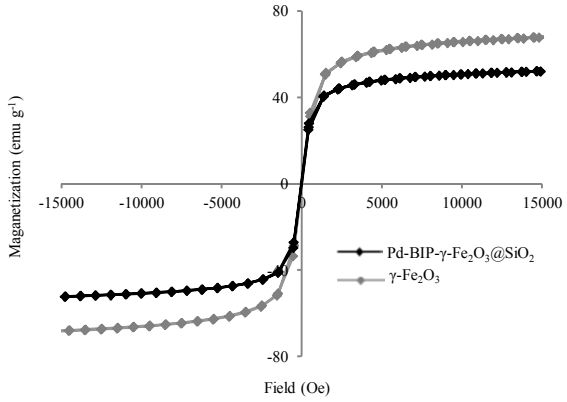

Figure 7. Magnetization curves of γ-Fe_2O_3 and Pd-BIP-γ-Fe_2O_3@SiO_2

Catalytic activity of Pd-BIP-γ-Fe_2O_3@SiO_2 in Heck, Suzuki and Sonogashira cross-coupling reactions

For optimization of the Heck coupling reaction conditions, we chose the coupling of iodobenzene (1 mmol) with *n*-butyl acrylate (1.1 mmol) in the presence of Pd-BIP-γ-Fe_2O_3@SiO_2 as a model reaction (Scheme 3).

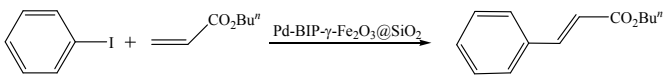

Scheme 3. Heck cross-coupling reaction of iodobenzene with *n*-butyl acrylate.

At first, the model reaction was performed in DMF at 100 °C in the presence of 0.25 and 0.5 mol% of Pd-BIP-γ-Fe_2O_3@SiO_2 and Et_3N (2 mmol) (Fig. 8a). In both reactions, the yield of the product was increased in 15 min and remains constant till 0.5 h. Higher yield was obtained in the presence of 0.5 mol% of the catalyst. The influence of a variety of solvents such as EtOH, CH_3CN, H_2O and toluene on the progress of the reaction were studied (Fig. 8b). Of the tested solvents, DMF was the best choice, giving the desired product in shorter reaction time (0.25 h) and with higher yield (98%) (Fig. 8b). A similar reaction under solvent-free conditions proceeded slowly in 1 h. In the screening of various bases, Et_3N gave the highest catalytic efficiency for this coupling reaction (Fig. 8c). The model reaction was also studied in the presence of Pd-BIP-γ-Fe_2O_3@SiO_2 (0.5 mol%) in DMF in 80 °C. The results of this study suggested that 100 °C is the optimum temperature for this reaction (Fig. 8d). The model reaction was examined in the absence of the catalyst, $Pd(OAc)_2$ and **2** (Fig. 8e). A trace amount of the product was obtained after 1 h in the absence of the catalyst. The catalytic activity of Pd-BIP-γ-Fe_2O_3@SiO_2 was higher than that of $Pd(OAc)_2$ and **2**.

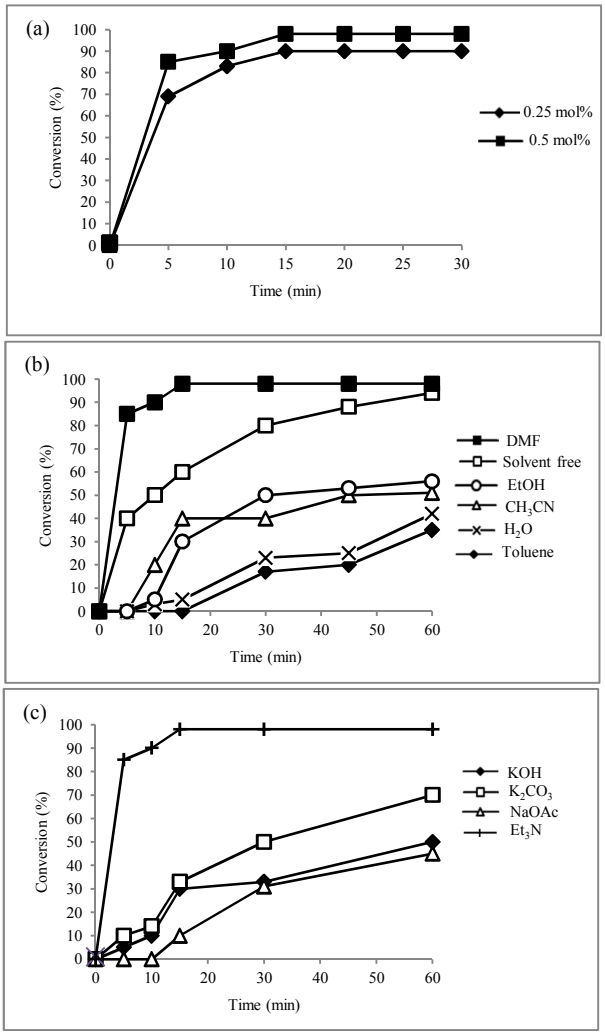

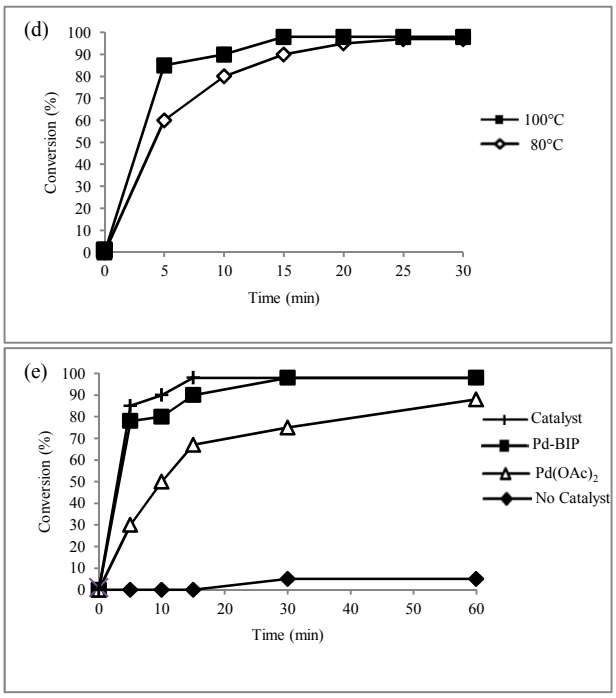

Figure 8. Effect of the amount of the catalyst (a), different bases (b), solvents (c), temperatures (d), and type of the catalyst (e) on reaction conversions.

To explore the scope of this method, the Heck coupling reaction of various aryl halides and olefins was studied under optimal reaction conditions (Table 1). Different aryl iodides reacted well with olefins including methyl/ethyl/*n*-butyl acrylate and the desired products were isolated in 86-98% yields (Entry 1-5). Aryl bromides reacted with *n*-butyl acrylate and generated the corresponding products in high yields (Entries 6-8). The applicability of this method for the coupling reaction of some aryl chlorides (far cheaper and more widely available than aryl iodides and bromides) with *n*-butyl acrylate was also examined. The examined aryl chlorides underwent the coupling reactions and gave the desired products in relatively good yields. However, the reaction proceeded in rather longer reaction times compared with aryl bromides and iodides (Entries 9-11). To test the potential for practical synthetic applications, a larger scale Heck coupling reaction of iodobenzene (50 mmol) with *n*-butyl acrylate (55 mmol) was carried out under the present reaction conditions. The reaction proceeded smoothly (2 h), giving 98% yield of the desired product.

It is worth to mention that $^{3}J_{H\text{-}H}$ value of 16.0-16.4 Hz for vinyllic hydrogens of the products was obtained using ^{1}H NMR spectra and showed an excellent selectivity for the formation of *trans* isomer of the products.

In order to extend the generality of this method, the Heck coupling reaction of aryl halides with styrene was also studied. The results showed that this catalytic system was effective for the Heck coupling reaction of styrene with both activated and deactivated aryl iodides, bromides and chlorides (Entries 12-19).

Table 1. Heck cross-coupling reaction of aryl halides with olefins using Pd-BIP-γ-Fe_2O_3@SiO_2

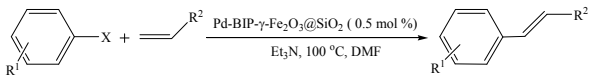

Entry	R^1	X	R^2	Time (h)	Yield[a] (%)
1	H	I	CO_2Bu^n	0.25	98
2	H	I	CO_2Me	0.75	95
3	H	I	CO_2Et	0.75	96
4	4-Cl	I	CO_2Bu^n	1.5	92
5	4-MeO	I	CO_2Bu^n	1.5	86
6	H	Br	CO_2Bu^n	4	92
7	4-NO_2	Br	CO_2Bu^n	2.5	92
8	4-CN	Br	CO_2Bu^n	3	90
9	H	Cl	CO_2Bu^n	5	83
10	4-CN	Cl	CO_2Bu^n	6	88
11	4-NO_2	Cl	CO_2Bu^n	6	91
12	H	I	Ph	2	90
13	4-Cl	I	Ph	3	88
14	4-MeO	I	Ph	3	80
15	H	Br	Ph	3.5	82
16	4-NO_2	Br	Ph	3	93
17	4-CN	Br	Ph	3	86
18	H	Cl	Ph	7	75
19	4-NO_2	Cl	Ph	7	75

[a]Isolated yield. Reaction conditions: aryl halide (1 mmol), olefin (1.1 mmol), Et_3N (2 mmol), Pd-BIP-γ-Fe_2O_3@SiO_2 (0.5 mol%), DMF, 100 °C. The products were characterized by comparison of their physical properties with the authentic samples.[6]

To check whether Pd was being leached out from the solid catalyst to the solution or weather the catalyst was truly heterogeneous in nature, Heck cross-coupling reaction of iodobenzene with *n*-butylacrylate was studied. After proceeding of 30% of the coupling reaction at 100 °C, the catalyst was separated by a magnet and the remaining solution was stirred for 12 h. In the absence of the catalyst, any increase in the conversion value (30%) was not detected. Moreover, ICP analysis of the remaining solution revealed that there was not any Pd in the reaction mixture. These results suggested that the Pd was not being leached out from the solid surface of the catalyst during coupling reaction and the catalyst was truly heterogeneous. Heterogeneous nature of the catalyst was further checked by employing a solid-phase poisoning test, by using 3-mercaptopropyl-functionalized γ-Fe_2O_3@SiO_2[16] as an efficient Pd scavenger. In a typical experimental procedure, iodobenzene (1 mmol), *n*-butyl acrylate (1.1 mmol), Et_3N (2 mmol) and DMF (10 ml) were mixed in a round bottom flask along with Pd-BIP-γ-Fe_2O_3@SiO_2 (0.02 g) and 3-mercaptopropyl-functionalized γ-Fe_2O_3@SiO_2 (0.05 g). The whole mixture was stirred in an oil bath for about 0.5 h at 100 °C. No change in the conversion was observed compared with the results obtained in the presence of Pd-BIP-γ-Fe_2O_3@SiO_2 (Table 1, entry 1). These results clearly demonstrated that this novel catalyst was heterogeneous in nature.

The reusability of the catalyst is a very important theme, especially for commercial and industrial applications. Therefore, the recovery and reusability of Pd-BIP-γ-Fe_2O_3@SiO_2 were investigated in the reaction of iodobenzene with *n*-butyl acrylate under the present reaction conditions. After the reaction was completed and allowed to be cooled, the catalyst was separated by a magnetic bar from the reaction mixture (Fig. 9b), washed with EtOAc, dried 30 min at 100 °C and reused for a consecutive run under the same reaction conditions. The catalyst was successfully used in 10 subsequent

reactions (Table 2). The average isolated yield of the product for ten consecutive runs was 93.1%, which clearly demonstrates the practical reusability of the catalyst. The average turnover number (TON = mmole of product/mmole of Pd catalyst) and average turnover frequency [TOF (h^{-1}) = TON/time] of the catalyst for 10 runs were 186 and 744 h^{-1}, respectively.

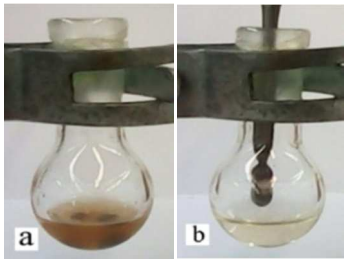

Figure 9. (a) Reaction mixture, (b) Separation of Pd-BIP-γ-Fe_2O_3@SiO_2 from the reaction mixture by a magnetic bar

Table 2. Recycling of Pd-BIP-γ-Fe_2O_3@SiO_2 for the Heck reaction of iodobenzene with *n*-butyl acrylate

Cycle	Yield[a] (%)	TON	TOF(h^{-1})
1st	98	196	784
2nd	98	196	784
3rd	98	196	784
4th	98	196	784
5th	96	192	768
6th	96	192	768
7th	92	184	736
8th	90	180	720
9th	85	170	680
10th	80	160	640

[a]Isolated yield. Reaction conditions: iodobenzene (1 mmol), *n*-butyl acrylate (1.1 mmol), Et_3N (2 mmol), Pd-BIP-γ-Fe_2O_3@SiO_2 (0.5 mol%), DMF, 100 °C, 0.25 h.

The TEM image of the catalyst after being reused ten times showed that the Pd nanoparticles were still well dispersed and no obvious aggregation of Pd was observed (Fig. 10).

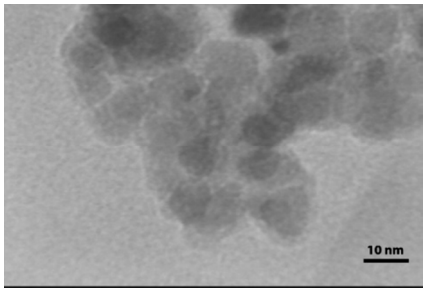

Figure 10. TEM of Pd-BIP-γ-Fe_2O_3@SiO_2 after tenth reuse

Comparison of FT-IR spectra of used catalyst (Fig. 11) with fresh catalyst demonstrates that the structure of the catalyst retained after first and tenth recoveries. Furthermore, the ICP and CHN analysis (N = 1.51% and C = 4.92%) of Pd-BIP-γ-Fe_2O_3@SiO_2 were carried out after ten times reuse and the results showed that only a very small amount (less than 1%) of Pd metal was removed from the catalyst.

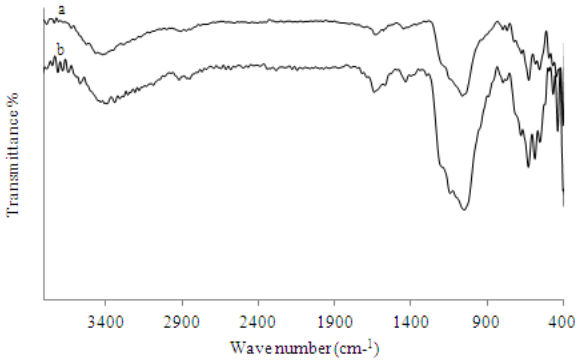

Figure 11. FT-IR spectra of Pd-BIP-γ-Fe_2O_3@SiO_2 after (a) first reuse, (b) tenth reuse

The activity of various recoverable palladium catalysts with Pd-BIP-γ-Fe_2O_3@SiO_2 in the Heck coupling reaction of *n*-butyl acrylate with iodobenzene was compared in Table 3. From Table 3, it is appeared that Pd-BIP-γ-Fe_2O_3@SiO_2 showed good catalytic activity for the Heck reactions in terms of TON and TOF compared with the other catalytic systems. More importantly, among supported palladium catalysts, our catalyst like the ones which were supported on magnetic nanoparticles could be easily separated from the reaction mixture by using an external magnet.

Table 3. Catalytic activity of Pd-BIP-γ-Fe_2O_3@SiO_2 compared with some recoverable catalysts reported for the Heck coupling reaction of *n*-butyl acrylate with iodobenzene

Entry	Catalyst (mol%)	Conditions	Yield[a] (%)[ref]	TON	TOF (h^{-1})
1	SiO_2@Fe_3O_4-Pd (1)	DMF, K_2CO_3, 100 °C, 8 h	97[18]	97	12
2	$PdCl_2$ (2.3) /DPPPEG[b] 200 (6.0)	Solvent free, Pr_3N, 80 °C, 5 min	95[19]	41	512
3	Si–PNHC[c]–Pd (0.5)	NMP, K_2CO_3, 120 °C, 2 h	95[20]	190	95
4	HMMS[d]-NH_2-Pd (4)	NMP, K_2CO_3, 130 °C, 8 h	98[21]	24	3
5	SMNPs[e]-supported 4,5-diazafluroen-9-one-Pd (1)	Solvent free, DABCO, 140 °C, 2 h	92[22]	92	46
6	$PdCl_2$/TiO_2 (0.5)	DMF, Et_3N, under 400 W (mercury vapor lamp) UV-visible irradiation 45±3 °C, 5 h	94[f23]	188	38
7	Fe_3O_4-NH_2-Pd (5)	NMP, K_2CO_3, 130 °C, 10 h	99<[g24]	20	2
8	Pd-DABCO-γ-Fe_2O_3 (1)	Solvent free, Et_3N, 100 °C, 0.5 h	92[25]	92	184
9	TiO_2@Pd NPs (1)	DMF, Et_3N, 140 °C, 10 h	92[26]	92	9
10	Pd-SMF[h] (1)	CH_3CN, Et_3N, 100 °C, 20 h	92[27]	92	5

11	Pd(0)–$ZnFe_2O_4$ (4.62)	DMF ,Et_3N, 120 °C, 3 h	90[28]	20	6
12	Pd-BIP-γ-Fe_2O_3@SiO_2 (0.5)	DMF, Et_3N, 100 °C, 0.25 h	98[i]	196	784

[a]Isolated yield.
[b]DPPPEG = bis-(diphenylphosphinite)PEG.
[c]PNHC = Polymeric N-heterocyclic carbene.
[d]HMMS = Monodispersed hollow magneticspheres.
[e]SMNPs = Silica-coated magnetite nanoparticles.
[f]Conversion.
[g]Determined by GC.
[h]SMF = Siliceous mesocellular foam.
[i]Current work.

Encouraged by the above results of Heck reactions, the catalytic activity of Pd-BIP-γ-Fe_2O_3@SiO_2 was then evaluated for Suzuki and Sonogashira coupling reactions (Tables 4 and 5). As shown in Tables 4 and 5, aryl halides (iodides, bromides and chlorides) functionalized with electron-withdrawing or electron-donating groups reacted with phenylboronic acid or phenyl acetylene to generate the corresponding products in good to high yields.

Table 4. Suzuki coupling reactions of aryl halides with phenylboronic acid using Pd-BIP-γ-Fe_2O_3@SiO_2

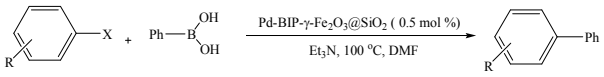

Entry	R	X	Time (h)	Yield[a] (%)
1	H	I	1	98
2	4-Cl	I	1.5	95
3	4-MeO	I	2	90
4	H	Br	3	92
5	4-MeO	Br	3	91
6	4-NO_2	Br	2.5	92
7	4-CN	Br	2.5	91
8	H	Cl	5	82
9	4-CN	Cl	4	86
10	4-NO_2	Cl	4	85

[a]Isolated yield. Reaction conditions: aryl halide (1 mmol), phenylboronic acid (1.1 mmol), Et_3N (2 mmol), Pd-BIP-γ-Fe_2O_3@SiO_2 (0.5 mol%), DMF, 100 °C. The products were characterized by comparison of their physical properties with the authentic samples.[29]

Table 5. Sonogashira coupling reaction of aryl halides with phenylacetylene using Pd-BIP-γ-Fe_2O_3@SiO_2

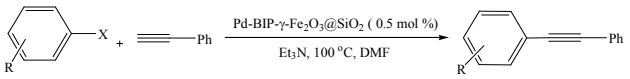

Entry	R	X	Time (h)	Yield[a] (%)
1	H	I	1.5	96
2	4-Cl	I	2.5	93
3	4-MeO	I	4	94
4	H	Br	4	90
5	4-MeO	Br	5	85
6	4-Me	Br	5	82
7	4-NO_2	Br	3	91
8	4-CN	Br	3	87
9	H	Cl	5	85
10	4-Me	Cl	6	71
11	4-CN	Cl	5	84
12	4-NO_2	Cl	5	82

[a]Isolated yield. Reaction conditions: aryl halide (1mmol), phenylacetylene (1.1 mmol), Et_3N (2 mmol), Pd-BIP-γ-Fe_2O_3@SiO_2 (0.5 mol%), DMF, 100°C. The products were characterized by comparison of their physical properties with the authentic samples.[30]

Conclusion

In summary, we have synthesized complex of Pd with bis(imino)pyridine as a NNN pincer ligand supported on γ-Fe_2O_3@SiO_2 magnetic nanoparticles (Pd-BIP-γ-Fe_2O_3@SiO_2). After its characterization by different methods, it was used a new air- and moisture-stable magnetically recyclable phosphine-free Pd catalyst for Heck, Suzuki and Sonogashira coupling reactions. A wide range of aryl halides (iodides, bromides and chlorides) was coupled successfully with alkyl acrylates, styrene, phenylboronic acid and phenylacetylene to generate the corresponding products in good to high yields. Any Pd detection in the remaining solution after separation of the catalyst in the hot filtration test and the results of poisoning test showed that the observed catalysis was heterogeneous in nature. The true heterogeneous Pd-BIP-γ-Fe_2O_3@SiO_2 could be reused by a magnetic bar for ten consecutive cycles without any drastic loss of its reactivity. Due to the true heterogeneous nature, simple and efficient recyclability and applicability for large scale coupling reactions, Pd-BIP-γ-Fe_2O_3@SiO_2 could be a potential catalyst for using in industrial chemistry. Further investigation on the application of Pd-BIP-γ-Fe_2O_3@SiO_2 in organic synthesis is underway in our laboratory.

Experimental

Generals

Chemicals were purchased from Merck Chemical Company. NMR spectra were recorded in ppm in $CDCl_3$ on a Bruker Advance DPX-400 and 250 instrument using TMS as internal standard. The purity of the products and the progress of the reactions were accomplished by TLC on silica-gel polygram SILG/UV254 plates. FT-IR spectra were recorded on a JASCO FT-IR 460 plus spectrophotometer. TEM analysis was performed using TEM microscope (Philips CM30). The morphology of the products was determined by using Hitachi Japan, model s4160 Scanning Electron Microscopy (SEM) at accelerating voltage of 15 KV. Thermo gravimetric analysis (TGA) was performed using a Shimadzu thermo gravimetric analyzer (TG-50). Elemental analysis was carried out on a Costech 4010 CHNS elemental analyzer. Power X- ray diffraction (XRD) was performed on aX'Pert Pro MPD diffractometer with Cu K_α (λ = 0.154 nm) radiation. Surface analysis spectroscopy of the catalyst was performed in an ESCA/AES system. This system was equipped with a concentric hemispherical (CHA) electron energy analyzer (Specs model EA10 plus) suitable for X-ray photoelectron spectroscopy (XPS). Room temperature magnetization isotherms were obtained using a vibrating sample magnetometer (VSM, Lake Shore 7400). The content of Pd in the catalyst was determined by OPTIMA 7300DV ICP analyzer.

Synthesis of amino-functionalized γ-Fe_2O_3@SiO_2

The γ-Fe_2O_3@SiO_2[14] (3.5 g) was sonicated in dry toluene (50 mL) for 30 min. (3-Aminopropyl)triethoxysilane (3.5 mL) was added to the dispersed γ-Fe_2O_3@SiO_2 in toluene, slowly heated to 105 °C and stirred at this temperature for 48 h. The resulting amino-functionalized γ-Fe_2O_3@SiO_2 was separated by an external magnet

and washed with toluene, ethanol-water mixture, deionized water and ethanol in turn, and dried under vacuum.

Synthesis of BIP supported on γ-Fe_2O_3@SiO_2

A solution of pyridine-2,6-dicarbaldehyde (15 mmol, 2.02 g) in methanol (20 mL) and amino-functionalized γ-Fe_2O_3@SiO_2 (1 g) was refluxed for 6 h at 60 °C. The resulting light brown solid was separated by an external magnet, repeatedly washed with hot methanol and finally dried in oven under vacuum.

Synthesis of the Pd-BIP-γ-Fe_2O_3@SiO_2

BIP supported on γ-Fe_2O_3@SiO_2 (1 g) was sonicated in methanol (30 mL) for 0.5 h. A solution of $Pd(OAc)_2$ (0.34 mmol, 0.076 g) in methanol (10 mL) was added to the dispersed BIP supported on γ-Fe_2O_3@SiO_2 in methanol and stirred under reflux for 10 h. The reaction mixture was cooled to room temperature. The solid was separated by an external magnet, washed several times with methanol and dried in an oven under vacuum.

Synthesis of 1

A solution of pyridine-2,6-dicarbaldehyde (15 mmol, 2.02 g) in methanol (20 mL) and (3-aminopropyl)triethoxysilane (30 mmol, 7.2 mL) was refluxed for 6 h. The resulting solid was separated, washed with hot methanol (3 × 10 mL) and finally dried in an oven under vacuum.

Synthesis of 2

A solution of $Pd(OAc)_2$ (0.34 mmol, 0.076 g) in methanol (10 mL) was added to **1** (0.34 mmol, 0.19 g) in methanol (10 mL) and stirred under reflux for 10 h. The reaction mixture was cooled to room temperature. The solid was separated, washed several times with methanol and dried in an oven under vacuum.

General procedure for the Heck, Suzuki and Sonogashira coupling reaction

A mixture of aryl halide (1.0 mmol), alkene/phenylboronic acid/phenylacetylene (1.1 mmol), Et_3N (2 mmol) and Pd-BIP-γ-Fe_2O_3@SiO_2 (0.018 g, 0.5 mol%) was stirred in DMF at 100 °C for an appropriate time (Tables 1, 4 and 5). After cooling the reaction mixture to room temperature, the catalyst was separated by a magnetic bar, washed several times with EtOAc, dried and reused for a new run. After evaporation of the solvent under vacuum, the crude product was subjected to silica gel column chromatography eluted with *n*-hexane/EtOAc (50/1) to afford the pure product.

(E)-n-Butyl cinnamate
^{1}H NMR (400 MHz, $CDCl_3$): δ 0.88 (t, 3H, ^3J = 7.6 Hz), 1.34-1.36 (m, 2H), 1.59-1.62 (m, 2H), 4.13 (t, 2H, ^3J = 6.8 Hz), 6.36 (d, 1H, ^3J = 16.0 Hz), 7.29-7.30 (m, 3H), 7.43-7.45 (m, 2H), 7.60 (d, 1H, ^3J = 16.4 Hz) ppm; ^{13}C NMR (100 MHz, $CDCl_3$), δ 13.7, 19.2, 30.8, 64.3, 118.2, 128.0, 128.8, 130.1, 134.4, 144.4, 166.8 ppm.
(E)-Methyl cinnamate
^{1}H NMR (400 MHz, $CDCl_3$): δ 3.74 (s, 3H), 6.38 (d, 1H, ^3J = 16.4 Hz), 7.31-7.33 (m, 3H), 7.45-7.47 (m, 2H), 7.63 (d, 1H, ^3J = 16.4 Hz) ppm; ^{13}C NMR (100 MHz, $CDCl_3$), δ 51.6, 117.7, 128.1, 128.9, 130.3, 134.3, 144.8, 167.3 ppm.
(E)-Ethyl cinnamate
^{1}H NMR (400 MHz, $CDCl_3$): δ 1.43 (t, 3H, ^3J = 8.0 Hz), 4.19 (q, 2H, ^3J = 8.0 Hz), 6.35 (d, 1H, ^3J = 16 Hz), 7.27-7.28 (m, 3H), 7.41-7.42 (m, 2H), 7.63 (d, 1H, ^3J = 16.0 Hz) ppm; ^{13}C NMR (100 MHz, $CDCl_3$), δ 14.2, 60.0, 118.2, 127.9, 128.7, 130.1, 134.3, 144.3, 166.6 ppm.
(E)-n-Butyl 3-(4-chlorophenyl)acrylate
^{1}H NMR (400 MHz, $CDCl_3$): δ 0.90 (t, 3H, ^3J = 7.2 Hz), 1.33-1.39 (m, 2H), 1.57-1.64 (m, 2H), 4.13 (t, 2H, ^3J = 6.8 Hz), 6.64 (d, 1H, ^3J = 16.0 Hz), 7.45 (d, 2H, ^3J = 8.0 Hz), 7.63 (d, 1H, ^3J = 16.0 Hz), 7.74 (d, 2H, ^3J = 8.0 Hz) ppm; ^{13}C NMR (100 MHz, $CDCl_3$), δ 13.7, 19.2, 30.7, 64.4, 118.8, 129.1, 129.4, 132.9, 136.0, 143.0, 166.7 ppm.
(E)-n-Butyl 3-(4-methoxyphenyl)acrylate
^{1}H NMR (400 MHz, $CDCl_3$): δ 0.91 (t, 3H, ^3J =7.0 Hz), 1.35-1.40 (m, 2H), 1.60-1.62 (m, 2H), 3.72 (s, 3H), 4.13 (m, 2H, ^3J =7.0 Hz), 6.24 (d, 1H, ^3J = 16.0 Hz), 6.81 (d, 3H, ^3J =4.8 Hz), 7.39 (d, 3H, ^3J =4.2 Hz), 7.58 (d, 1H, ^3J = 16.0 Hz) ppm; ^{13}C NMR (100 MHz, $CDCl_3$), δ 13.6, 19.1, 30.7, 55.0, 64.0, 114.1, 115.5, 127.0, 129.5, 144.0, 161.2, 167.1 ppm.
(E)-n-Butyl 3-(4-nitrophenyl)acrylate
^{1}H NMR (400 MHz, $CDCl_3$): δ 0.92 (t, 3H, ^3J = 7.2 Hz), 1.35-1.44 (m, 2H), 1.62-1.69 (m, 2H), 4.17-4.24 (m, 2H), 6.53 (d, 1H, ^3J = 16.0 Hz), 7.63-7.68 (m, 3H), 8.20 (d, 2H, ^3J = 8.0 Hz) ppm; ^{13}C NMR (100 MHz, $CDCl_3$), δ 13.6, 19.1, 30.6, 64.7, 122.5, 124.0, 128.6, 140.5, 141.5, 148.3, 166.0 ppm.
(E)-n-Butyl 3-(4-cyanophenyl)acrylate
^{1}H NMR (400 MHz, $CDCl_3$): δ 0.77 (t, 3H, ^3J = 7.0 Hz), 1.30-1.38 (m, 2H), 1.57-1.64 (m, 2H), 4.14 (t, 2H, ^3J = 6.8 Hz), 6.45 (d, 1H, ^3J = 16.0 Hz), 7.54 (d, 2H, ^3J = 8.4 Hz), 7.60 (d, 2H, ^3J = 8.0 Hz) ppm; ^{13}C NMR (100 MHz, $CDCl_3$), δ 13.5, 19.0, 30.5, 64.4, 113.0, 118.1, 121.6, 128.3, 132.4, 138.4, 141.8, 165.7 ppm.
(E)-1,2-Diphenylethene
^{1}H NMR (400 MHz, $CDCl_3$): δ 7.18 (s, 2H), 7.33 (t, 2H, ^3J = 6.8 Hz), 7.42 (t, 4H, ^3J = 7.0 Hz), 7.58 (d, 4H, ^3J = 7.2 Hz) ppm; ^{13}C NMR (100 MHz, $CDCl_3$), δ 126.7, 127.8, 128.8, 137.4 ppm.
(E)-1-Chloro-4-styrylbenzene
^{1}H NMR (400 MHz, $CDCl_3$): δ 7.07 (s, 2H), 7.28-7.39 (m, 5H), 7.43-7.46 (m, 2H), 7.50-7.52 (m, 2H) ppm; ^{13}C NMR (100 MHz, $CDCl_3$), δ 127.7, 128.5, 128.8, 129.0, 129.9, 130.0, 130.4, 134.3, 136.9, 138.1 ppm.
(E)-1-Methoxy-4-styrylbenzene
^{1}H NMR (400 MHz, $CDCl_3$): δ 3.89 (s, 3H), 6.92 (d, 2H, ^3J = 8.4 Hz), 6.99 (d, 2H, ^3J = 16.4 Hz), 7.09 (d, 2H, ^3J = 16.0 Hz), 7.36 (t, 2H, ^3J = 7.6 Hz), 7.46-7.52 (m, 3H), ppm; ^{13}C NMR (100 MHz, $CDCl_3$), δ 55.3, 114.1, 126.3, 126.6, 127.2, 127.8, 128.2, 128.7, 130.1, 137.7, 159.3 ppm.
(E)-1-Nitro-4-styrylbenzene
^{1}H NMR (400 MHz, $CDCl_3$): δ 7.06-7.18 (m, 1H), 7.40-7.45 (m, 4H), 7.49-766 (m, 4H), 8.15-8.26 (m, 2H) ppm; ^{13}C NMR (100 MHz, $CDCl_3$), δ 125.2, 127.4, 128.0, 128.2, 130.0, 134.4, 137.3, 145.0, 147.8 ppm.
(E)-4-Styrylbenzonitrile
^{1}H NMR (400 MHz, $CDCl_3$): δ 7.09 (d, 1H, ^3J = 16.0 Hz), 7.22 (d, 1H, ^3J = 16.0 Hz), 7.31-7.34 (t, 1H, ^3J = 4.0 Hz), 7.38-7.41 (t, 2H, ^3J = 4.0 Hz), 7.54 (d, 2H, ^3J = 7.2 Hz), 7.58 (d, 2H, ^3J = 8.4 Hz), 7.64 (d, 2H, ^3J = 8.4 Hz) ppm; ^{13}C NMR (100 MHz, $CDCl_3$), δ 111.7, 120.2, 127.8, 128.0, 128.1, 129.8, 130.0, 133.5, 133.6, 137.4, 142.9 ppm.
Biphenyl
^{1}H NMR (400 MHz, $CDCl_3$): δ 7.46 (t, 2H, ^3J = 7.2 Hz), 7.56 (t, 4H, ^3J = 8.0 Hz), 7.72 (d, 4H, ^3J = 6.8 Hz) ppm; ^{13}C NMR (100 MHz, $CDCl_3$), δ 127.2, 127.3, 128.8, 141.3 ppm.
4-Chlorobiphenyl
^{1}H NMR (400 MHz, $CDCl_3$): δ 7.31-7.49 (m, 5H), 7.51-7.57 (m, 4H) ppm; ^{13}C NMR (100 MHz, $CDCl_3$), δ 128.1, 128.7, 129.3, 129.5, 130.0, 130.2, 140.8, 141.1 ppm.
4-Methoxybiphenyl

^{1}H NMR (400 MHz, $CDCl_3$): δ 3.83 (s, 3H), 6.99 (d, 2H, ^3J = 8.8 Hz), 7.31 (t, 1H, ^3J = 7.2 Hz), 7.43 (t, 2H, ^3J = 8.0 Hz), 7.55 (t, 4H, ^3J = 8.8 Hz) ppm; ^{13}C NMR (100 MHz, $CDCl_3$), δ 56.5, 115.3, 127.8, 127.9, 129.3, 129.9, 134.9, 142.0, 160.3 ppm.

4-Nitrobiphenyl

^{1}H NMR (400 MHz, $CDCl_3$): δ 7.43-7.52 (m, 3H), 7.62-7.64 (m, 2H), 7.73-7.76 (m, 2H), 8.29-8.30 (m, 2H) ppm; ^{13}C NMR (100 MHz, $CDCl_3$), δ 125.2, 128.5, 128.9, 130.0, 130.3, 139.9, 148.2, 148.7 ppm.

4-Cyanobiphenyl

^{1}H NMR (400 MHz, $CDCl_3$):δ 7.41-7.51 (m, 3H), 7.56-7.60 (m, 2H), 7.68-7.74 (m, 4H), ppm; ^{13}C NMR (100 MHz, $CDCl_3$), δ 112.0, 120.1, 128.3, 128.8, 129.8, 130.2, 133.7, 140.3, 146.8 ppm.

1,2-Diphenylethyne

^{1}H NMR (400 MHz, $CDCl_3$): δ 7.27 (t, 6H, ^3J = 7.5 Hz), 7.34-7.43 (m, 4H) ppm; ^{13}C NMR (100 MHz, $CDCl_3$) δ 89.3, 123.2, 128.2, 128.4, 131.6 ppm.

1-Methoxy-4-phenylethynyl-benzene

^{1}H NMR (400 MHz, $CDCl_3$): δ 3.86 (s, 3H), 6.92 (d, 2H, ^3J = 8.8 Hz), 7.35-7.41 (m, 3H), 7.53 (d, 4H, ^3J = 7.2 Hz), 7.56-7.58 (m, 2H) ppm; ^{13}C NMR (100 MHz, $CDCl_3$) δ 55.3, 88.1, 89.4, 114.0, 115.4, 123.6, 127.9, 128.3, 131.5, 133.1, 159.6 ppm.

1-Methyl-4-phenylethynyl-benzene

^{1}H NMR (250 MHz, $CDCl_3$): δ 2.27 (s, 3H), 7.04-7.46 (m, 9H).

Heck coupling reaction of iodobenzene and *n*-butyl acrylate in large scale

A mixture of iodobenzene (50 mmol), *n*-butyl acrylate (55 mmol), Et_3N (100 mmol), and Pd-BIP-γ-Fe_2O_3@SiO_2 (0.9 g, 0.5 mol%) was stirred in DMF at 100 °C. After completion, the reaction mixture was cooled to room temperature and the catalyst was separated by a magnetic bar. The solvent was evaporated under vacuum and the crude product was subjected to silica gel column chromatography eluted with *n*-hexane/EtOAc (50/1) to afford the pure product in 98% yield.

Acknowledgement

Financial support of this project by University of Birjand Research Council is appreciated.

References

[a]*Address, Department of Chemistry, College of Sciences, University of Birjand, Birjand, Iran. Fax: +98 56 32202065; Tel: +98 5632202065; E-mail: ssobhani@birjand.ac.ir, sobhanisara@yahoo.com*

[1] M. Gholinejad, V. Karimkhani, I. Kim, *Appl .Organomet. Chem.*, 2014, **28**, 221; R.J. Lundgren, M. Stradiotto, *Chem. Eur. J.*, 2012, **18**, 9758; I. P. Beletskaya, A. V. Cheprakov, *Chem. Rev.*, 2000, **100**, 3009; N. J. Whitcombe, K. K. Hii, S. E. Gibson, *Tetrahedron*, 2001, **57**, 7449; A. F. Littke, G. C. Fu, *Angew. Chem. Int. Ed.*, 2002, **41**, 4176.

[2] V. Polshettiwar, A. Molnár, *Tetrahedron*, 2007, **63**, 6949; A. Zamboulis, N. Moitra, J. J .E. Moreau, X. Cattoën, M. Wong Chi Man, *J. Mater. Chem.*, 2010, **20**, 9322.

[3] R. A. Gossage, H. A. Jenkins, P. N. Yadav, *Tetrahedron Lett.*, 2004, **45**, 7689.

[4] T. S. Phan, M. Van Der Sluys, C W. Jones, *Adv. Synth. Catal.*, 2006, **348**, 609; R. Martin, S. L. Buchwald, *Chem. Res.*, 2008, **41,** 1461.

[5] X-Q. Zhang, Y-P. Qiu, B. Rao, M-M. Luo, *Organometallics*, 2009, **28,** 3093; B. P. Morgan, G. A. Galdamez, R. J. Gilliard, R. C. Smith, *Dalton Trans*., 2009, 2020; Y-B. Zhou, Z-X. Xi, W-Z. Chen, D-Q. Wang, *Organometallics*, 2008, **27,** 5911.

[6] M. Bakherad, S. Jajarmi, *J. Mol. Catal. A Chem.*, 2013, **370**, 152; D. Wang, D. Denux, J. Ruiz, D. Astruc, *Adv. Synth. Catal.*, 2013, **355**, 129; M. Bakherad, A. Keivanloo, B. Bahramian, S. Jajarmi, *J. Organomet. Chem.*, 2013, **724**, 206.

[7] C. Uerpmann, B. J. L. Henner, C. Guérin, F. Carre, *J. Organomet. Chem.,* 2005, **690**, 197; T. V. Laine, M. Klinga, M. Leskela, Eur. *J. Inorg. Chem*., 1999, **1999**, 959; K. T. Sylvester, P. J. Chirik, *J. Am. Chem. Soc.*, 2009, **131**, 8772.

[8] B. L. Small, M. Brookhart, A. M. A. Bennett, *J. Am. Chem. Soc.*, 1998, **120**, 4049; R. Duchateau, *Chem. Rev.,* 2002, **102**, 3525.

[9] A. J. Canty, J. Patel, B. W. Skelton, A. H. White, *J. Organomet. Chem.,* 2000, **607**, 194.

[10] M. E. van der Boom, D. Milstein, *Chem. Rev.*, 2003, **103**, 1759; W. Leis, H. A. Mayer, W. C. Kaska, Coord. *Chem. Rev.*, 2008, **252**, 1787; J. Takaya, N. Iwasawa, *Organometallics*, 2009, **28**, 6636; J. I. van der Vlugt, *Angew. Chem. Int. Ed*., 2010, **49**, 252.

[11] K. Dhara, K. Sarkar, D. Srimani, S. K. Saha, P. Chattopadhyay, A. Bhaumik, *Dalton Trans.*, 2010, **39**, 6395.

[12] N. E. Leadbeater, M. Marco, *Chem. Rev*., 2002, **102**, 3217; S. Minakata, M. Komatsu, *Chem. Rev*., 2009, **109**, 711; M. Kaur, H. Zhang, Y. Qiang, *IEEE Magn. Lett*., 2013, **4**, 4000204; M. Kaur, A. Johnson, G. Tian, W. Jiang, L. Rao, A. Paszczynski, Y. Qiang, *Nano Energy*, 2013, **2**, 124; R. B. Nasir Baig, R. S. Varma, *Chem Commun*., 2013, **49**, 752; R. Mrówczyński, A. Nan, J. Liebscher, *RSC Adv.,* 2014, **4**, 5927.

[13] Sh. Wang, Z. Zhang, B. Liu, J. Li, *Catal. Sci. Technol*., 2013, **3,** 2104.

[14] A. P. Philipse, M. P. B. van Bruggen, C. Pathmamanoharan, *Langmuir*, 1994, **10**, 92; Q. Liu, Z. Xu, J. A. Finch, R. Egerton, *Chem. Mater*., 1998, **10**, 3936; X. Q. Liu, Z. Y. Ma, J. M. Xing, H. Z. Liu, *J. Magn. Magn. Mater.*, 2004, **270**, 1.

[15] S. Sobhani, S. Rezazadeh, *Synlett*, 2010, 1485; R. Malakooti, S. Sobhani, N. Razavi, S. Shafiei, R. Mokhtari, Collect. Czech. *Chem. Commun.*, 2011, **76**, 1979; S. Sobhani, S. Rezazadeh, *J. Iran. Chem. Soc.*, 2011, **8**, 198; S. Sobhani, Z. Pakdin-Parizi, S. Rezazadeh, *J. Organomet. Chem.*, 2011, **696**, 813; S. Sobhani, Z. Pakdin-Parizi, N. Razavi, *Appl. Catal. A: Gen.*, 2011, **410**, 162; S. Sobhani, R. Jahanshahi, *New J. Chem.*, 2013, **37**, 1009; S. Sobhani, Z. Pakdin-Parizi, R. Naseri, *J. Chem. Sci.*, 2013, **125**, 975; S. Sobhani, M. S. Ghasemzadeh, M. Honarmand, F. Zarifi, *RSC Adv.*, 2014, **4**, 44166; S. Sobhani, Z. Vahidi, Z. Zeraatkar, S. Khodadadi, *RSC Adv.*, 2015, **5**, 36552.

[16] S. Sobhani, M. Bazrafshan, A. ArabshahiDelluei, Z. Pakdin-Parizi, *Appl. Catal. A: Gen.*, 2013, **454**, 145.

[17] F. Heshmatpour, R. Abazari, S. Balalaie, *Tetrahedron*, 2012, **68**, 3001.

[18] P. Li, L. Wang, L. Zhang, G-W. Wang, *Adv. Synth. Catal*., 2012, **354**, 1307.

[19] N. Iranpoor, H. Firouzabadi, A. Riazi, A. Shakerpoor, *Appl. Organometal. Chem*., 2013, **27**, 451.

[20] B. Tamami, F. Farjadian, S. Ghasemi, H. Allahyari, *New J. Chem*., 2013, **37**, 2011.

[21] P. Wang, H. Liu, M. Liu, R. Li, J, Ma. *New J. Chem*., 2014, **38**, 1138.

[22] M. A. Zolfigol, T. Azadbakht, V. Khakyzadeh, R. Nejatyami, D. M. Perrin, *RSC Adv*., 2014, **4**, 40036.

[23] S. B. Waghmode, S. S. Arbuj, B. N. Wani, *New J. Chem*., 2013, **37**, 2911.

[24] F. Zhang, J. Jin, X. Zhong, S. Li, J. Niu, R. Li, J. Ma, *Green Chem*., 2011, **13**, 1238.

[25] S. Sobhani, Z. Pakdin Parizi, *Appl. Catal. A: Gen*., 2014, **479**, 112.

[26] M. Nasrollahzadeh, A. Azarian, A. Ehsani, M. Khalaj, *J. Mol. Catal. A Chem*., 2014, **394**, 205.

[27] N. Erathodiyil, S. Ooi, A. M. Seayad, Y. Han, S. S. Lee, J. Y. Ying, *Chem.-Eur. J*., 2008, **14**, 3118.

[28] A. S. Singh, U. B. Patil, J. M. Nagarkar, *Catal. Commun*., 2013, **35**, 11.

[29] H. Firouzabadi, N. Iranpoor, S. Motevalli, M. Talebi, *J Organomet. Chem.,* 2012, **118**, 708; A. Modak, J. Mondal, A. Bhaumik, *Green Chem.*, 2012, **14** ,2840.

[30] R. Bernini, S. Cacchi, G. Fabrizi, G. Forte, F, Petrucci, A. Prastaro, S. Niembro, A. Shafir, A. Vallribera, *Green Chem.,* 2010, **12**, 150; P. Li, L. Wang, L. Zang, G-W. Wang, *Adv. Synth.Catal*., 2012, **354**, 1307; A. Modak, J. Mondal, M. Sasidharan, A. Bhaumik, *Green Chem.*, 2011, **13**, 1317; A. S. Paraskar, A. Sudalai, *Tetrahedron*, 2006, **62**,

4907; F. Lopes, R. Moreira, T. Rodrigues, *Synthetic Commun.*, 2012, **42**, 747.

